Computer Assisted Mechanics and Engineering Sciences, 6: 63–82, 1999.

Criteria for chaotic transient oscillations in a model of driven buckled beams

Wanda Szemplińska-Stupnicka, Elżbieta Tyrkiel and Andrzej Zubrzycki
Institute of Fundamental Technological Research
Polish Academy of Sciences
Świętokrzyska 21, 00-049 Warszaw, Poland

(Received March 24, 1988)

The single-mode equation of motion of a class of buckled beams is considered, and the attention is focused on the phenomena of irregular, unpredictable transient oscillations which are observed in the region of the nonlinear resonance hysteresis. This type of transient motion may be dangerous in engineering dynamics, because it may last very long and is defined neither by the coefficient of damping nor by the magnitude of perturbation. While the steady-state chaotic motion has been studied extensively in the recent literature, little attention was paid to the chaotic transients. In the paper the criteria for transient chaos, i.e. the domain of the system control parameter values, where the chaotic transient motion can occur, are determined. The criteria are based on the theoretical concept of global bifurcations, and are estimated numerically.

1. INTRODUCTION

If a dissipative vibrating system is driven by a periodic force, it is expected that the steady-state response is also periodic and that a transient motion, induced by a perturbation of the steady-state, is strictly defined by the damping force and the magnitude of perturbation. When Tseng and Dugundji [23] published in 1971 their results of an experiment on a lateral vibration of a buckled beam, and obtained a random-like, irregular steady-state response, it was rather interpreted as a result of some "noise" in realization of the experiment, than a discovery of a new nonlinear phenomena.

Although at that time the phenomena of chaotic motion in deterministic dynamical systems were already studied extensively in mathematical physics, and also were observed in a mathematical model of atmospheric turbulence [7], crucial publications relevant to mechanical systems did not appear until the year of 1979. Then the series of papers on the subject appeared, which covered all aspects of the problem that were essential for engineering oriented people; occurrence of the chaotic motion in deterministic dissipative mechanical system was presented by performing physical experiments, and was studied theoretically by considering a single-mode equation of motion from a theoretical point of view, and verified by an analog computer [5, 9, 10, 12].

Since that time the theoretical and computational aspects of the new, strongly nonlinear phenomena, were studied extensively by a number of authors, and the list of the references would be extremely large indeed; we refer the reader to some of them, published in book form: [3, 4, 11, 14, 21, 27].

The aim of this paper is twofold: we want to present the aspects of the occurrence of chaotic motion which are relevant to safe engineering, and also to draw an attention of the engineers to the theoretical and numerical aspects of the problem which are useful in establishing the criteria for the system control parameters values. We exemplify the problem by the use of a mathematical model of a buckled beam under lateral excitation.

In the studied model the nonlinearity that gives rise to the nonlinear phenomena is due to large displacements and belongs to the category of geometric nonlinearity. In the light of the recently developed theory of chaos in dissipative dynamical systems [14], the original equations of motions of the continuous systems need to be reduced to the three-dimensional dynamical system with continuous time, that is to the set of 3 autonomous, first order differential equations of motion:

$$\frac{d\bar{z}}{dt} = \bar{f}(z), \qquad \bar{z} = (z_1, z_2, z_3). \tag{1}$$

In our example the dynamical system takes the form of the nonautonomous, second order ordinary differential equation:

$$\ddot{x} + h\dot{x} + \alpha_0 x + \alpha_2 x^2 + \alpha_3 x^3 = F\cos\omega t, \tag{2}$$

where: $x \equiv z_1$, $\dot{x} \equiv z_2$, $\omega t \equiv z_3$.

At this point it is essential to refer to the question of adequacy of the reduction of the continuous system, described originally by the partial integro-differential equations, to the Eqs. (1), (2). We briefly note that the reduction has two aspects: it has been proved that the essence of the chaotic phenomena is usually captured by the three dimensional dynamical system and, from the other hand, the relevant theorems that enable us to perform appropriate quantitative numerical analysis, are also confined to the three-dimensional dynamical system. A detail consideration of the problem can be found in books which include the center manifold theorem, e.g. [3].

In engineering practice, it is a common assumption that if the eigenvalues (i.e. the natural frequencies of a linearized system) are incommensurable, the sufficient approximation is obtained by a single-mode motion approach, that is, by assuming that the displacement $v(z,t)$ can be written as:

$$v(z,t) = \Psi(z)x(t),$$

where $\Psi(z)$ is a properly selected eigenfunction (usually the fundamental one if the driving frequency ω is not too high). Then the standard Galerkin projection method is applied, and the effects of the higher modes are neglected.

Central to understanding the chaotic motion properties is the concept of *maps*. For continuous motions (flows), this amounts to discrete time sampling of the motion in the phase space. For the periodically driven oscillators considered, it is common to use the period of excitation $T = 2\pi/\omega$ as the sampling time. The map thus obtained can be viewed as a stroboscopic image of the system response and it allows us to reduce the dimension of the phase space from 3 to 2 and to present the results on the phase plane. The stroboscopic picture of the motion in the phase space $x(nT) - \dot{x}(nT)$, synchronous with the forcing function, is called a "*Poincaré map*".

For the stroboscopic picture of x (or $\dot{x}$) versus a selected forcing parameter (F or ω) — the term *bifurcation diagram* is adopted.

The same idea is applied for visualization the basins of attraction of coexisting *attractors* (i.e. steady-state stable solutions, periodic or chaotic). We recall that the *basin of attraction* of an attracting set is defined by the domain of all initial conditions $(x(0), \dot{x}(0))$ in the phase plane whose trajectories approach asymptotically that attracting set. It is important to notice, that there are the coexisting unstable solutions (*saddles*), which, although physically unrealizable, play an important role in basin organization: the stable invariant manifolds (insets) of the saddles are the lines which separate domains of attraction of the coexisting attractors. With the increase of the forcing parameter the boundaries of the basins of attraction undergo relevant changes from a regular (smooth) structure to a more complicated *fractal structure*, i.e. highly intertwined, fine-scale structure with a fractional (non-integer) dimension greater than 1 (e.g. [8, 14]). The concept of the fractal structure of basins of attraction of coexisting attractors is central to understanding the most essential property of chaotic motion: the *sensitivity to initial conditions*. The metamorphoses of the structure of basins' boundaries and, in particular, their various fractal patterns, are governed by the underlying geometric structure — the intersection of the stable and unstable invariant manifolds of one or more

coexisting unstable periodic orbits (saddles). This type of relevant changes in the global topology of the phase space belongs to the category of *global (homoclinic and heteroclinic) bifurcations* [3, 14, 25, 26]. Computation of the threshold values of the system control parameters, for which the global bifurcations occur, enables us to determine the regions of the system parameters, for which the system becomes chaotic, that is, for which a random-like, unpredictable motion can appear.

All these geometric and qualitative properties of the chaotic system dynamics require numerical computations, and presentation of the results needs the use of high quality color computer graphics. For instance, computing basins of attraction we create a grid of boxes (with an assumed resolution) covering the screen, which represents the phase plane $(x, \dot{x})$. Numerical procedure fills a grid box with an assumed color if the trajectory of its center converges, after a predefined number of iterations, to the particular attractor.

In the paper we first briefly outline a derivation of the single-mode equation of motion of a buckled beam subject to lateral external periodic excitation. The system belongs to the category of oscillators with two stable equilibrium positions at $F = 0$ (the twin-well potential system of Duffing type) and is so rich in various, inherently nonlinear phenomena, that it gives a good opportunity to present multiple aspects of the problems of the modern nonlinear dynamics, and to draw attention on the adequate methods of investigation.

The main purpose of the paper, however, is to determine the criteria for the transient chaotic motion, that is the critical system control parameters which give rise to random-like, unpredictable and, consequently, dangerous oscillations in the region of the primary resonance. The major investigation, computational results and discussion on multiple aspects of the chaotic transients and the related indeterminate outcomes are presented in Sec. 5.

Numerical results presented in the paper were obtained with the use of the computer program *Dynamics*, which accompanies the book [13]. Most of the data were run with a Runge-Kutta solver of order 4, with 95 steps per cycle (we also run some data with higher numbers of steps per cycle, but the results were almost identical).

2. Mathematical model of a class of buckled beams

The twin-well potential Duffing system studied in the paper has a mathematical relevance as the simplified model of a buckled beam undergoing forced, lateral vibrations. The partial integro-differential equation governing such motion, obtained by a standard method, can be written in a nondimensional form as [6]:

$$\ddot{v} + v'''' + \delta\dot{v} + H_0 v'' - k\left\{\int_0^1 [v'(\xi)]^2 d\xi\right\} v'' = \bar{F}(z,t), \tag{3}$$

where $v(z,t)$ is the lateral deflection, a prime denotes differentiating by z, and a dot – differentiating by t, δ represents viscous damping, k denotes the nonlinear membrane stiffness, and H_0 stands for the axial compressive load applied to the beam.

The nonlinear term expresses the fact that the axial force in the beam increases with lateral deflection, leading to increasing restoring force. We assume that H_0 is higher that the first Euler load, $H_0 > H_{\mathrm{cr}}^1$, so that the beam takes up a stable buckled state when the lateral force $\bar{F}(z,t)$ is zero.

By representing the displacement by the linear eigenfunction $\Psi(z)$ and considering a monofrequent harmonic excitation with a given spatial distribution $\Phi(z)$:

$$v = \Psi(z)u(t), \qquad \bar{F}(z,t) = \Phi(z) f \cos\bar{\omega}t, \tag{4}$$

and applying the conventional Galerkin projection method, we obtain a single ordinary differential equation of motion:

$$\ddot{u} + k\dot{u} - \alpha u + \beta u^3 = A\cos\bar{\omega}t, \qquad \alpha, \beta > 0, \tag{5}$$

where A is the amplitude of the generalized force:

$$A = \int_0^1 \Phi(z)\Psi(z)f\,dz,$$

and the generalized mass equals 1.

The single-mode equation of motion (5) was first derived for beams with simply supported boundaries and the buckling induced by the axial compressive load. Then it was shown that the same equation governs the single-mode lateral oscillations of a wide class of beams with various boundary conditions, and buckling induced also by different than the axial load mechanisms [12, 23].

For the sake of generality we reduce the equation (5) to the standard form:

$$\ddot{x} + h\dot{x} - \frac{1}{2}x + \frac{1}{2}x^3 = F\cos\omega t, \tag{6}$$

where:

$$t = \tau\Omega_0, \qquad \omega = \frac{\bar{\omega}}{\Omega_0}, \qquad x = u\sqrt{\frac{\beta}{\alpha}}, \qquad h = \frac{k}{\Omega_0}, \qquad F = \frac{A}{\Omega_0^2}\sqrt{\frac{\beta}{\alpha}}, \qquad \Omega_0 = \sqrt{2\alpha},$$

and Ω_0 is the linear natural frequency of oscillations around the stable, buckled position.

The standard system (6) satisfies the condition, that the two stable (buckled) equilibrium positions are located at $x_{1,2}^0 = \pm 1$, the unstable equilibrium position corresponds to $x = 0$, and the natural frequency $\Omega_0 = 1$.

3. Periodic and chaotic oscillations in the twin-well potential driven oscillator — preliminaries

In this paper the twin-well potential system (6) has been derived as a simple mathematical model of the single-mode motion of buckled beams driven externally by a lateral harmonic force. It is worthwhile to recall, however, that the system has become a central archetypal model for studies of chaos and fractal basin boundaries in nonlinear dynamics, the studies being still continued by applied mathematicians and physicists in various branches of physics.

For the sake of simplicity it is useful to interpret the system behavior as a motion of a ball (mass point) in the twin well potential, with the base vibrating harmonically (Fig. 1a). The ball can oscillate around one of the two stable positions, i.e. can exhibit *single-well motion*, or, at certain values of the system control parameters F, ω, it can leave the potential well and oscillate around all three equilibria to exhibit *cross-well motion* (chaotic or periodic).

To derive an equation of the single-well motion it is useful to introduce a new coordinate $z = x \pm 1$,which denotes the displacement from the stable rest position $x = \pm 1$. It follows that after the change of variables, Eq. (6) is transformed into:

$$\ddot{z} + h\dot{z} + z \mp \frac{3}{2}z^2 + \frac{1}{2}z^3 = F\cos\omega t. \tag{7}$$

It is known that the steady-state cross-well motion (chaotic or periodic) occurs at high values of the forcing parameter F. In this paper we focus attention on the system behavior at lower values of F, the values which seem to be of interest in real engineering problems. In practice the most dangerous and hence the most interesting phenomena occur in the region of the *primary resonance*, i.e. in *the neighborhood of the driving frequency* $\omega = 1$, where the *nonlinear resonance hysteresis* occurs. It follows that within each of the potential wells two stable T-periodic oscillations (resonant and nonresonant) coexist. This is schematically illustrated in Fig. 1b, where the closed trajectories

of the solutions are depicted in the phase-space $x - \dot{x}$. On the Poincaré map these T-periodic trajectories are reduced to stable fixed points: S_n', S_r' and S_n'', S_r'' denote nonresonant and resonant stable periodic orbits (attractors) in the left and the right potential well, respectively. The related unstable T-periodic orbits, i.e. *single-well saddles* (dashed trajectories) are reduced to unstable fixed points D' and D''. The Poincaré map of the unstable T-periodic solution that occurs close to $x = 0$ is denoted D_H and is called the *hill-top saddle.*

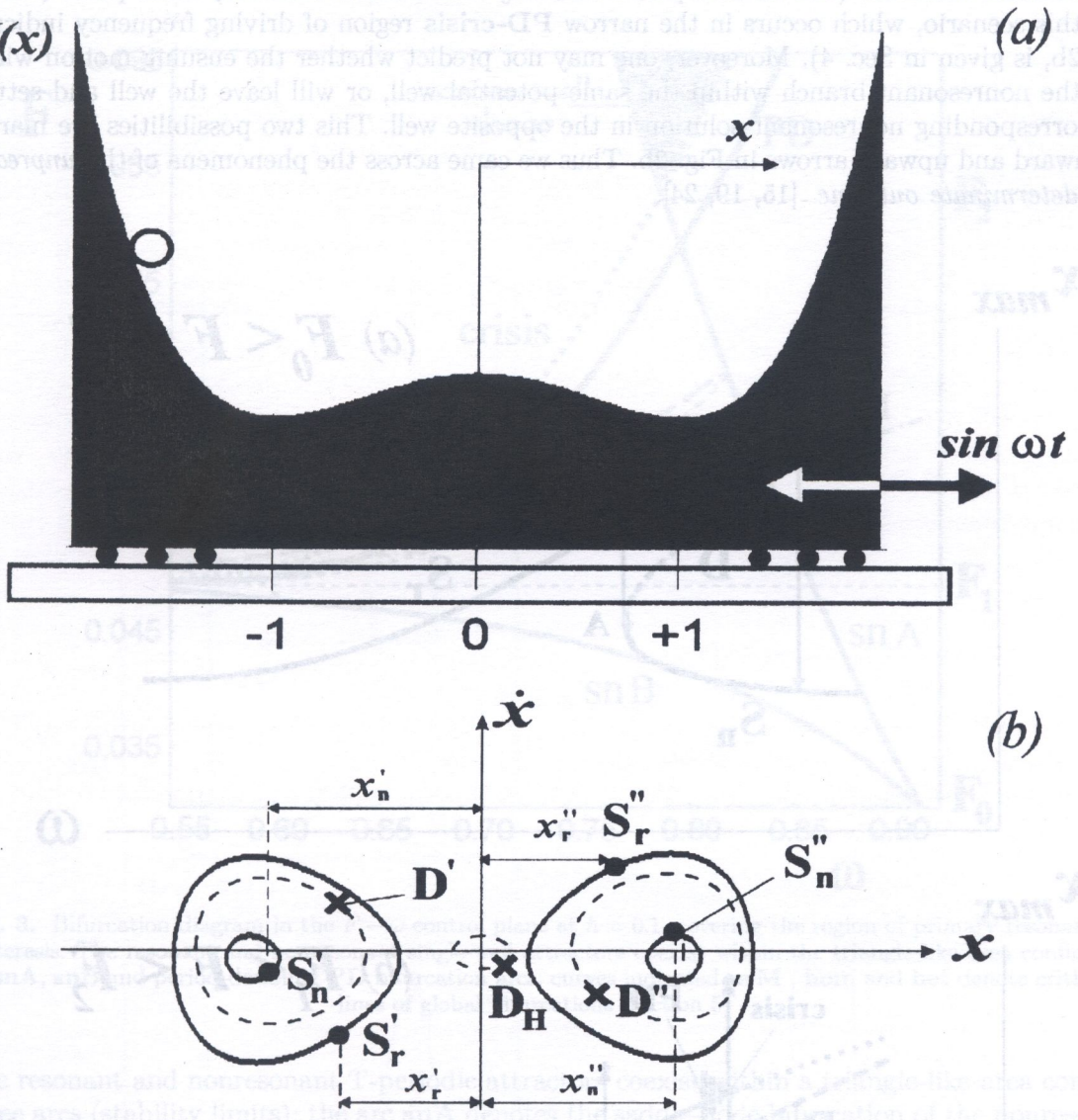

Fig. 1. (a) Schematic diagram of the potential energy of the system; (b) Coexistence of resonant and nonresonant T-periodic single-well oscillations: S_r' , S_r'' – resonant attractors; S_n' , S_n'' - nonresonant attractors; D', D'' - unstable single-well orbits (saddles); D_H - hilltop saddle

At very low values of the forcing parameter F ($F_0 < F < F_1$) the system behaves as a *weakly nonlinear* oscillator with a softening characteristic of restoring force. The steady-state response is very close to a harmonic one with frequency ω, and the amplitude-frequency curves skew towards the lower frequencies than that of the linear natural frequency $\Omega_0 = 1$ (Fig. 2a). The upper stable branch of the curve corresponds to the resonant attractor, the lower branch – to the nonresonant one. The two stable solutions are separated by the unstable one (dashed line) – this corresponds to the in-well saddle D in Fig. 1b. The nonlinear resonance hysteresis occurs between the two stability

limits **A** and **B** (saddle-node bifurcations). At the stability limits the *jump* phenomena is observed, but the resulting motion is always confined to the same potential well.

Yet the approximate theory gives a good agreement with the numerical results within a very slim zone of the forcing parameter F. At higher values of F ($F_1 < F < F_2$) the steady-state solution obtained by computer based methods begins to reveal some irregular and unpredictable behavior. In Fig. 2b we indicate schematically two aspects of the phenomena. First, we see that the saddle-node bifurcation **B** ceases to exist and instead another mechanism of the annihilation of the resonant attractor (known as a *period-doubling–chaos–crisis* scenario) takes place (an insight into this scenario, which occurs in the narrow **PD-crisis** region of driving frequency indicated in Fig. 2b, is given in Sec. 4). Moreover, one may not predict whether the ensuing motion will jump into the nonresonant branch within the same potential well, or will leave the well and settle into the corresponding nonresonant solution in the opposite well. This two possibilities are marked by downward and upward arrows in Fig. 2b. Thus we came across the phenomena of the *unpredictable* or *indeterminate outcome* [15, 19, 24].

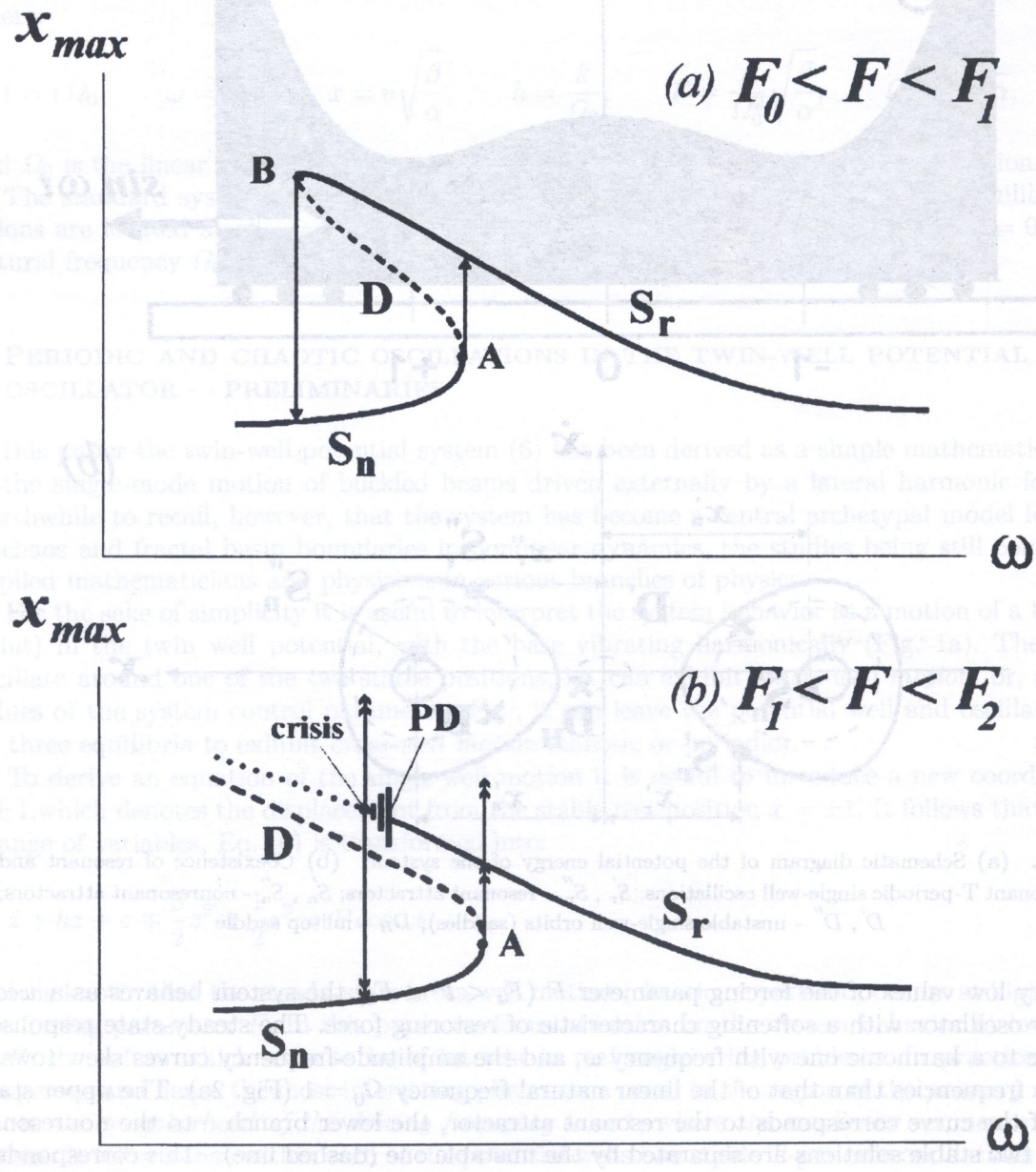

Fig. 2. Schematic amplitude-frequency curves in two regions of the forcing amplitude F

4. Steady-state oscillations in the region of the primary resonance hysteresis

To examine the asymptotic behavior of the system in the region of the primary resonance hysteresis we first determine the region of existence of the resonant and nonresonant T-periodic attractors, and then focus on the bifurcations which occur at the boundaries of the coexistence of the two attractors. The results are presented in the system parameter control plane $F-\omega$ at fixed value of damping $h = 0.1$ (Fig. 3).

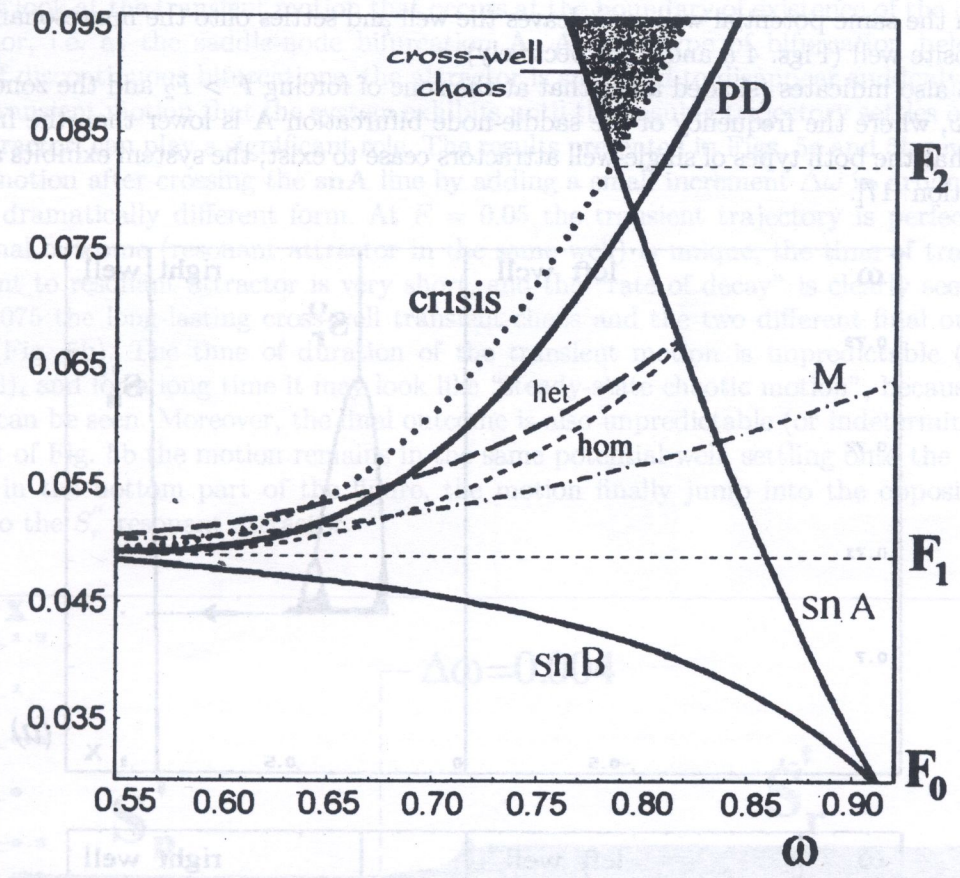

Fig. 3. Bifurcation diagram in the $F-\omega$ control plane at $h = 0.1$, covering the region of primary resonance hysteresis. The resonant and nonresonant single-well attractors coexist within the triangle-like area confined by **snA**, **snB** and period-doubling **PD** bifurcation arcs; curves indicated as **M** , **hom** and **het** denote critical lines of global bifurcations (section 5)

The resonant and nonresonant T-periodic attractors coexist within a triangle-like area confined by three arcs (stability limits): the arc **snA** denotes the saddle-node bifurcation of the nonresonant attractor S_n, the arc **snB** — the saddle-node bifurcation of the resonant attractor S_r. Finally, the arc **PD** depicts the first period-doubling bifurcation of the resonant attractor S_r. The points indicating the local saddle-node bifurcations **A** and **B** are already shown in the amplitude-frequency diagram in Fig. 2a, and the period-doubling bifurcation **PD** is also marked schematically in the Fig. 2b. The diagram in Fig. 2b suggests, that as the saddle-node bifurcation **snB** ceases to exist, the strict loss of stability of the resonant attractor S_r is followed by some irregular phenomena. The bifurcation diagram $x_P \equiv x_P(\omega)$ (where x_P denotes the Poincaré displacement on the Poincaré section plane) gives an insight into the sequence of bifurcations which occur in a narrow region between the arcs **PD** and **crisis** (Fig. 4). The diagram was obtained by decreasing the driving frequency ω, starting from the interior of the triangle-like area and crossing the values of ω, where the attractor ceases to exist. The diagram indicates, that the final annihilation of the resonant attractor is preceded

by a *cascade of the Feigenbaum period-doubling bifurcations*, the cascade which was found in many physical systems, and which is regarded in nonlinear dynamics as a generic route to chaos [1]. At the end of the cascade the single-well steady-state chaos (*chaotic attractor*) is observed in a very narrow band of the driving frequency, and this attractor is finally annihilated by a mechanism of a *boundary crisis*, i.e. the collision of the chaotic attractor with a coexisting saddle in its basin boundary [2, 16, 22]. In this paper we do not enter into details of this type of chaos. The two versions of the bifurcation diagram are mainly aimed at illustrating also another irregular phenomenon – the indeterminate final outcome. We see, that under a small increment of the forcing parameter F ($\Delta F = 0.0001$) the system, after annihilation of the chaotic attractor, settles onto the nonresonant attractor in the same potential well, or it leaves the well and settles onto the nonresonant attractor in the opposite well (Figs. 4 a and b, respectively).

Figure 3 also indicates (shaded area) that at the zone of forcing $F > F_2$ and the zone of driving frequency ω, where the frequency of the saddle-node bifurcation **A** is lower than the frequency of **crisis,** so that the both types of single-well attractors cease to exist, the system exhibits a cross-well chaotic motion [17].

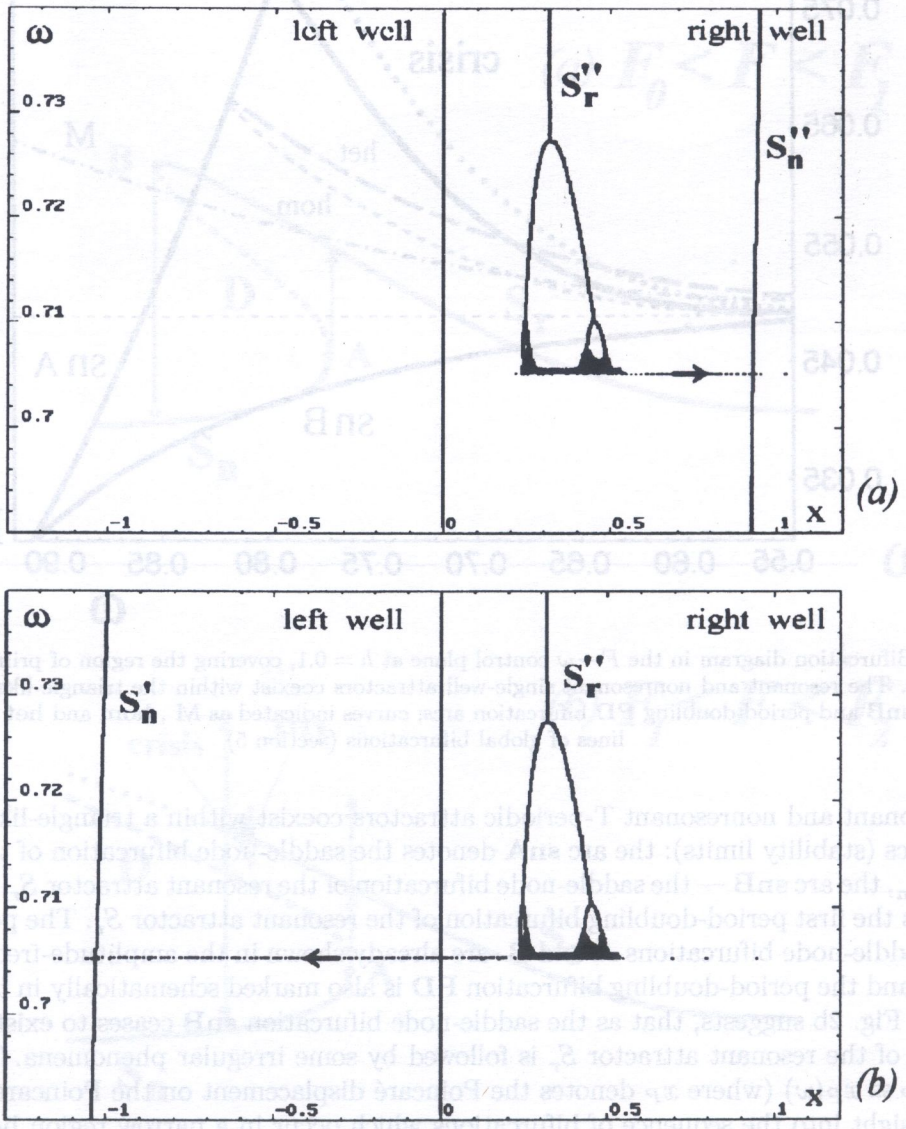

Fig. 4. Bifurcation diagrams of the resonant right-well attractor S_r'' and two possible outcomes after crisis (to the same or to the opposite well), under small step-increments of driving force: (a) $F = 0.0620$; (b) $F = 0.0621$

5. CRITERIA FOR CHAOTIC TRANSIENT MOTION

In this section we consider the transient chaotic motion that occurs in the region of the primary resonance, and focus on establishing criteria for the system parameter critical values F, ω, which define the boundary between regular and chaotic motion. We show that the transient chaotic motion can be induced by two different mechanisms: one mechanism is related to a "disturbance" applied to the steady-state periodic motion, and the other is due to a "disturbance" of the control parameter values F, ω at the strict loss of stability of the periodic motion, the disturbance that results in an annihilation of one of the coexisting attractors.

First we look at the transient motion that occurs at the boundary of existence of the nonresonant S_n attractor, i.e. at the saddle-node bifurcation **A**. As this type of bifurcation belongs to the category of discontinuous bifurcations, the attractor is supposed to disappear suddenly at $\omega = \omega_A$. If so, the transient motion that the system exhibits until the ensuing trajectory settles onto another remote attractor, can play a significant role. The results presented in Figs. 5a and 5b reveal that the transient motion after crossing the **snA** line by adding a small increment $\Delta\omega$ in driving frequency may have dramatically different form. At $F = 0.05$ the transient trajectory is perfectly regular, and the final outcome (resonant attractor in the same well) is unique; the time of transient from nonresonant to resonant attractor is very short, and the "rate of decay" is clearly seen (Fig. 5a). At $F = 0.075$ the long-lasting cross-well transient chaos and the two different final outcomes are observed (Fig. 5b). The time of duration of the transient motion is unpredictable (can not be established), and for a long time it may look like "steady-state chaotic motion", because any "rate of decay" can be seen. Moreover, the final outcome is also unpredictable (or indeterminate); in the upper part of Fig. 5b the motion remains in the same potential well, settling onto the S'_r resonant attractor; in the bottom part of the figure, the motion finally jump into the opposite well and settles onto the S''_r resonant attractor.

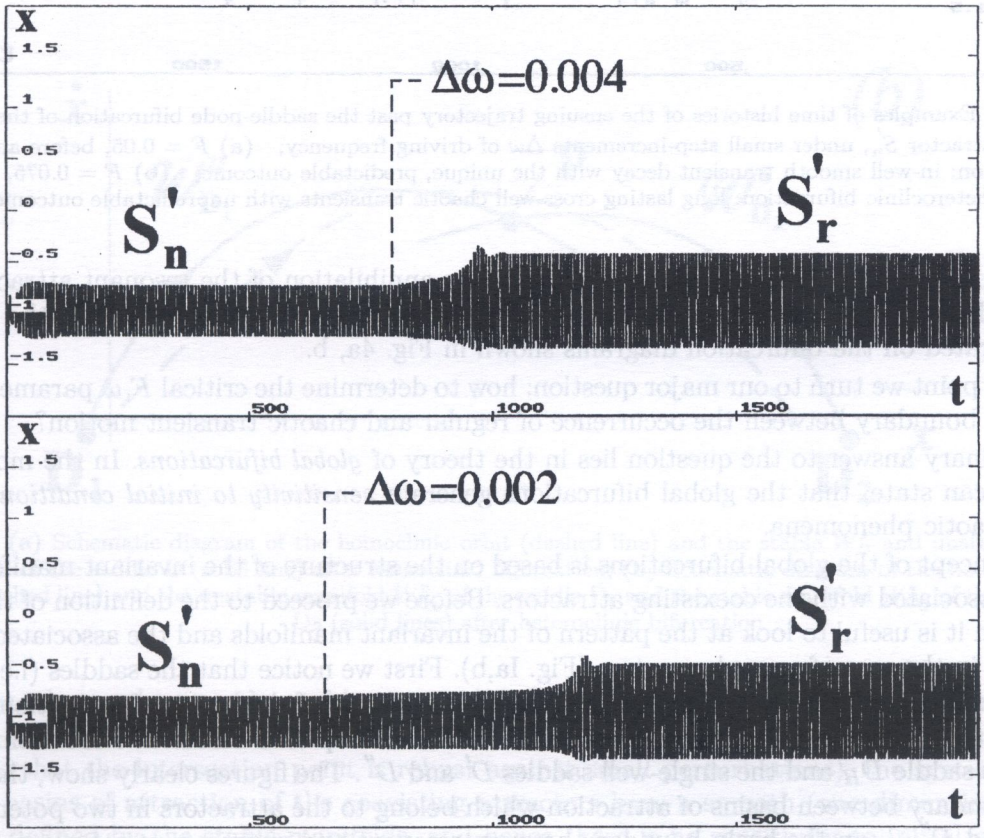

[Fig. 5a]

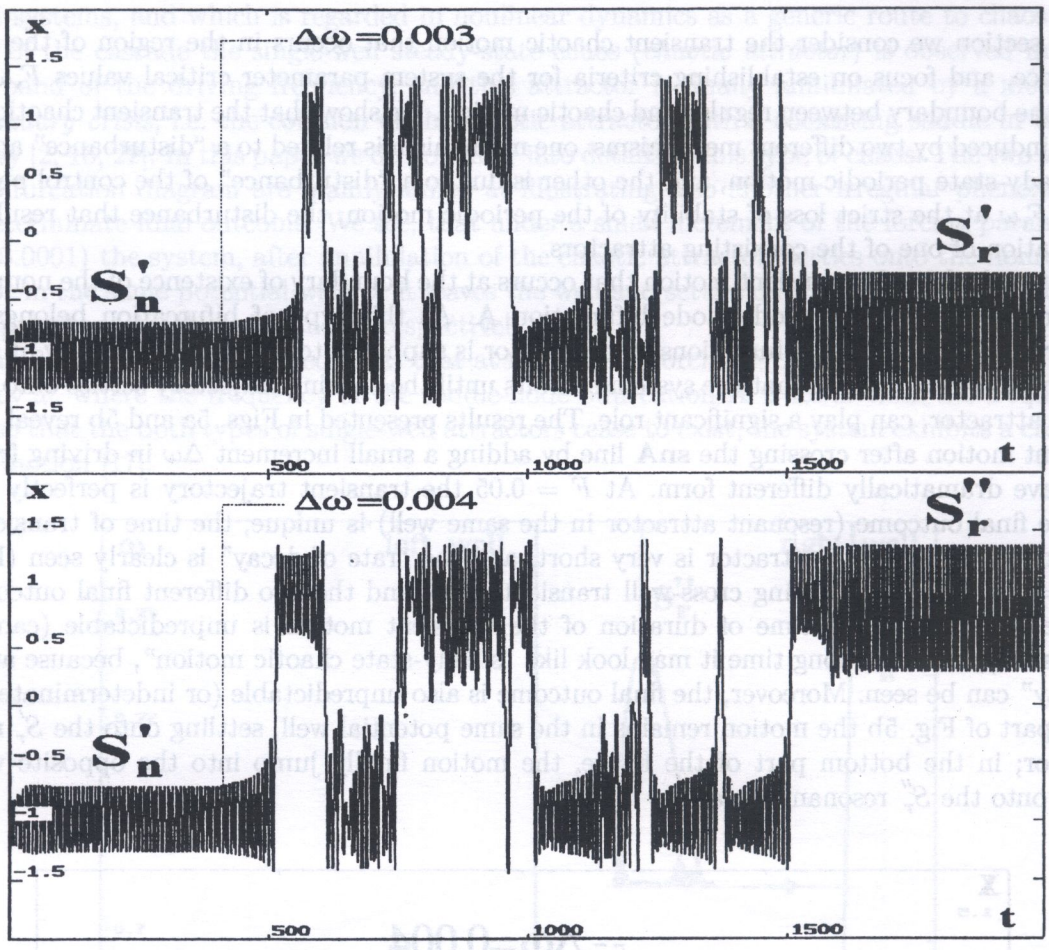

Fig. 5. Examples of time histories of the ensuing trajectory past the saddle-node bifurcation of the nonresonant attractor S_n', under small step-increments $\Delta\omega$ of driving frequency; **(a)** $F = 0.05$, before any global bifurcation: in-well smooth transient decay with the unique, predictable outcome; **(b)** $F = 0.075$, past the heteroclinic bifurcation: long lasting cross-well chaotic transients with unpredictable outcomes

The indeterminate outcomes may also occur after annihilation of the resonant attractor S_r via the cascade of period-doublings and crisis of the single-well chaotic attractor [19]; the event was just illustrated on the bifurcation diagrams shown in Fig. 4a, b.

At this point we turn to our major question: how to determine the critical F, ω parameters which define the boundary between the occurrence of regular and chaotic transient motion?

Preliminary answer to the question lies in the theory of *global bifurcations*. In the most general term one can state, that the global bifurcations generate *sensitivity to initial conditions* and this implies chaotic phenomena.

The concept of the global bifurcations is based on the structure of the invariant manifolds of the saddles, associated with the coexisting attractors. Before we proceed to the definition of this type of bifurcation it is useful to look at the pattern of the invariant manifolds and the associated basins of attraction in the case of a regular system (Fig. Ia,b). First we notice that the saddles (i.e. Poincaré map of unstable periodic orbits) are situated at the boundaries of the basins of attraction, and that the boundaries are smooth, one dimensional lines. In this example we deal with 3 coexisting saddles: the hilltop saddle D_H and the single-well saddles D' and D''. The figures clearly show, that D_H lies in the boundary between basins of attraction which belong to the attractors in two potential wells, and D' and D'' — on the basin boundary between resonant and nonresonant attractor within the same well.

When we compare the boundaries of the basins of attraction with the invariant manifolds of the 3 saddles D_H, D' and D'', we notice immediately that the boundaries are defined by the *stable manifolds (insets)*, i.e. the sets of initial points which tend to the saddle as $t \to \infty$ (for the sake of clarity, in Fig. Ib we show only short, most relevant segments of the invariant manifolds, corresponding to a short time of numerical integration).

Then we proceed to the concept of the global bifurcations and the role they play in our problem. The major events that define global bifurcations are schematically illustrated in Fig. 6a,b. The

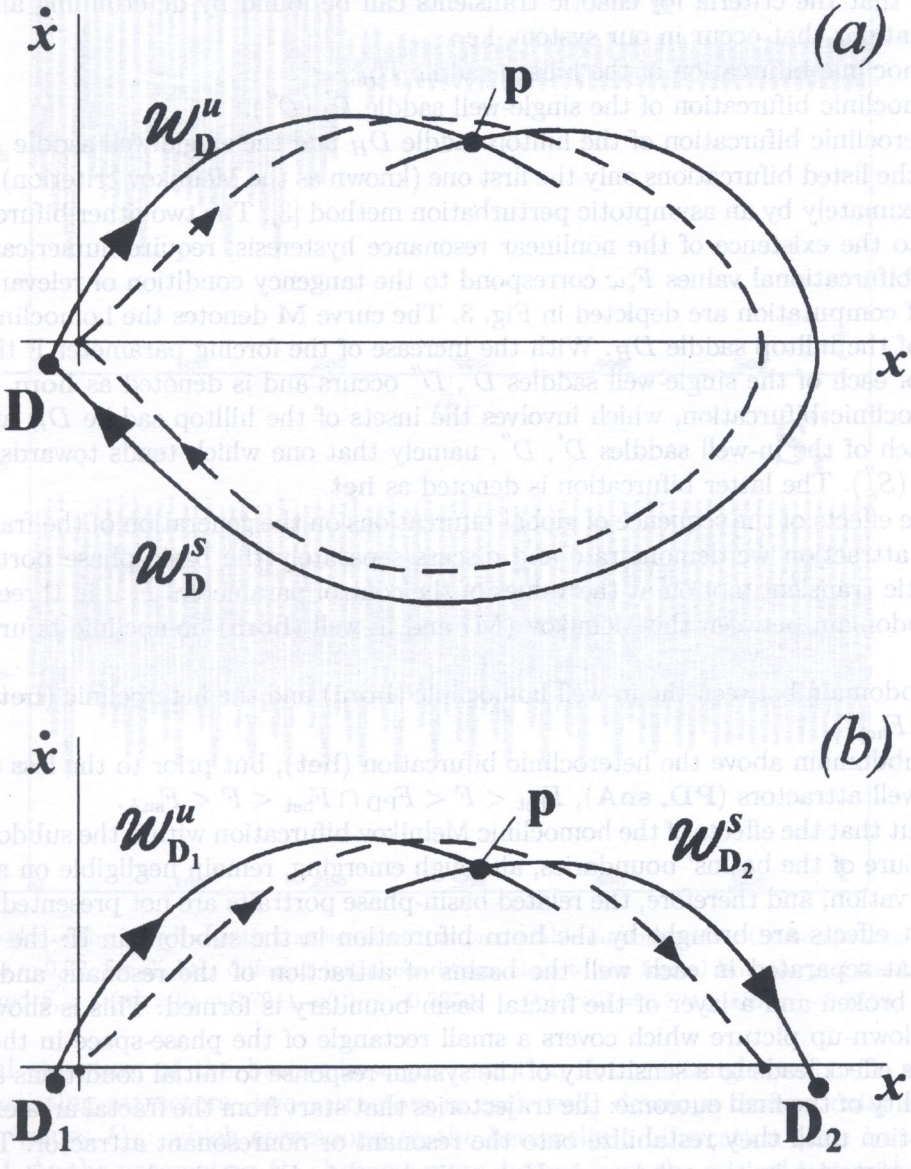

Fig. 6. (a) Schematic diagram of the homoclinic orbit (dashed line) and the stable W^s_D and unstable W^u_D manifolds of the saddle D (solid line) after homoclinic bifurcation; (b) Schematic diagram of the heteroclinic orbit (dashed line) and the unstable manifold $W^u_{D_1}$ of the saddle D_1 and the stable manifold $W^s_{D_2}$ of the saddle D_2 (solid lines) after heteroclinic bifurcation

theory says, that as long as the stable manifold W^s_D and unstable manifold W^u_D of the saddle D (or of the two saddles D_1 and D_2) do not intersect transversely (*transversal*, or *generic, intersection* means that the intersection point is robust against small perturbations), the system behaves regularly: basins of attraction of the coexisting attractors have a smooth (one dimensional) basin boundary, defined by the stable manifolds, and hence there is no sensitivity to initial conditions. The homoclinic (or heteroclinic) bifurcation occurs when the two manifolds (stable and unstable)

of the same saddle (or of the two different saddles, respectively) intersect transversely in the phase space. It is also known from the theory that one intersection implies infinite number of them (it results from the fact that the manifolds are invariant subspaces) and, consequently, infinite number of unstable orbits. This destroys the regular boundary between basins of attraction of the two coexisting attractors in the system, and the basin boundary becomes fractal. In the domain where the fractal nature of the basin boundaries occurs, the system is sensitive to initial conditions. In this sense the system becomes chaotic.

It follows that the criteria for chaotic transients can be found by determining all types of the global bifurcations that occur in our system, i.e.:

- the homoclinic bifurcation of the hilltop saddle D_H;
- the homoclinic bifurcation of the single-well saddle D' (D'');
- the heteroclinic bifurcation of the hilltop saddle D_H and the single well saddle D' (D'').

Between the listed bifurcations only the first one (known as the Melnikov criterion) can be determined approximately by an asymptotic perturbation method [3]. The two other bifurcations, which are related to the existence of the nonlinear resonance hysteresis, require numerical exploration. The critical bifurcational values F, ω correspond to the tangency condition of relevant manifolds.

Results of computation are depicted in Fig. 3. The curve **M** denotes the homoclinic (Melnikov) bifurcation of the hilltop saddle D_H. With the increase of the forcing parameter F the homoclinic bifurcation of each of the single-well saddles D', D'' occurs and is denoted as **hom**. It is followed by the heteroclinic bifurcation, which involves the insets of the hilltop saddle D_H and one of the outsets of each of the in-well saddles D', D'', namely that one which tends towards the resonant attractor S'_r (S''_r). The latter bifurcation is denoted as **het**.

To explore effects of the sequence of global bifurcations on the generation of the fractal structure of basins of attraction we demonstrate and discuss separately the basin-phase portraits and the related chaotic transient motion at the values of the control parameters F, ω in three subdomains:

I. the subdomain between the Melnikov (**M**) and in-well (**hom**) homoclinic bifurcation, $F_{\mathrm{M}} < F < F_{\mathrm{hom}}$;

II. the subdomain between the in-well homoclinic (**hom**) and the heteroclinic (**het**) bifurcation, $F_{\mathrm{hom}} < F < F_{\mathrm{het}}$;

III. the subdomain above the heteroclinic bifurcation (**het**), but prior to the loss of stability of both single-well attractors (**PD**, **snA**), $F_{\mathrm{het}} < F < F_{\mathrm{PD}} \cap F_{\mathrm{het}} < F < F_{\mathrm{snA}}$.

It turns out that the effects of the homoclinic Melnikov bifurcation within the subdomain I on the fractal structure of the basins' boundaries, although emerging, remain negligible on a macroscopic level of observation, and therefore, the related basin-phase portraits are not presented in the paper.

Significant effects are brought by the **hom** bifurcation in the subdomain II: the regular basin boundary that separated in each well the basins of attraction of the resonant and nonresonant attractors is broken and a layer of the fractal basin boundary is formed. This is shown in Fig. IIa and in the blown-up picture which covers a small rectangle of the phase-space in the right well – Fig. IIb. This effect leads to a sensitivity of the system response to initial conditions and so, to the unpredictability of the final outcome: the trajectories that start from the fractal area exhibit chaotic transient motion until they restabilize onto the resonant or nonresonant attractor. Two examples of such time histories in the subdomain II are displayed in Fig. 7a,b; they are obtained for sets of slightly different initial conditions in the close neighborhood of the fractal basin boundary in the right well ($x(0) \approx 0.79$, $\dot{x}(0) \approx -0.37$). Note, that this type of chaotic transient is confined to the motion within a single potential well and, therefore, the phenomenon is not restricted to the twin-well potential oscillator.

For the comparison we show in Fig. 8a,b two examples of transient trajectories which initialize in the phase plane very close to the former ones, but in the smooth (non-fractal) domains of the basins of S''_n (Fig. 8a) and S''_r (Fig. 8b) attractors; the trajectories reach the corresponding attractors after significantly shorter and more regular transients.

One may expect that due to the Melnikov homoclinic bifurcation the system has also a possibility of generating the cross-well transient chaos. But the fractal layer of the basin boundary which

involves the basins of attractors from both potential wells is so thin (and situated close to the edges of the basins), that this type of transients is neglected in the subdomain considered.

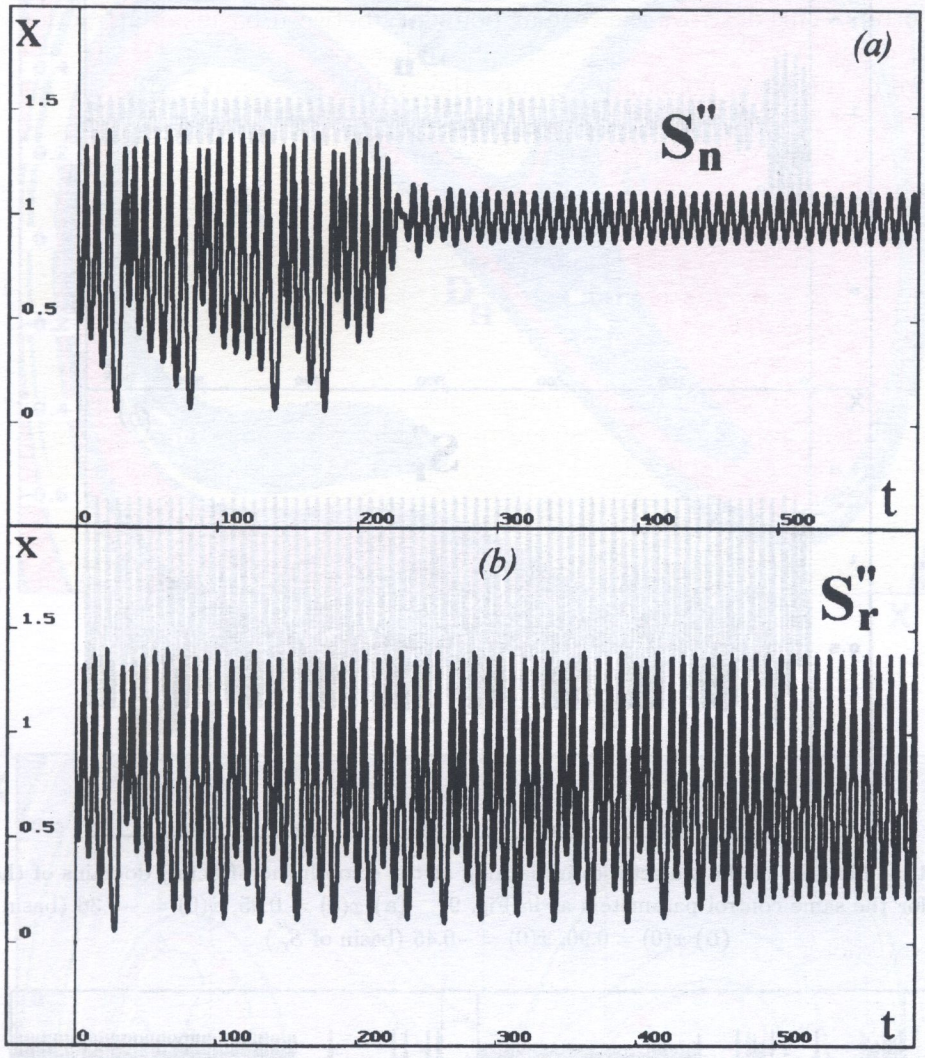

Fig. 7. Samples of the in-well chaotic transients with unpredictable outcomes after the homoclinic bifurcation, $F = 0.058$, $\omega = 0.72$, for slightly different initial conditions close to the fractal boundary of the basins of S''_r and S''_n: **(a)** $x(0) = 0.7941$, $\dot{x}(0) = -0.3770$; **(b)** $x(0) = 0.7941$, $\dot{x}(0) = -0.3768$

The fractal structure of the basin-phase portrait that form a tangled mixture of the basins of all four coexisting attractors (two attractors in each well) develops dramatically after crossing the threshold values F, ω which correspond to the heteroclinic bifurcation (line **het** in Fig. 3) – subdomain III. As the parameters F, ω become more distant from the critical **het** values, the effects of the heteroclinic bifurcation are growing, that is, the subset of initial conditions corresponding to the fractal domain of the basins is increasing, and gradually begins to cover a significant area of the phase space $x(0) - \dot{x}(0)$. To highlight the effect we display the basins of attraction for the forcing parameter value $F = 0.075$, which significantly exceeds the critical F_{het} threshold, but still remains within the triangle-like domain where all four periodic attractors coexist (Fig. III). In this case, the highly intertwined structure of the basins gives rise to cross-well chaotic transients, which can result in as many as four different final outcomes. Four examples of the time history of chaotic transients which settle finally onto each of the four coexisting attractors, are displayed in Fig. 9. They are obtained for sets of slightly different initial conditions in the close neighborhood of $x(0) = 0.11$, $\dot{x}(0) = -0.009$.

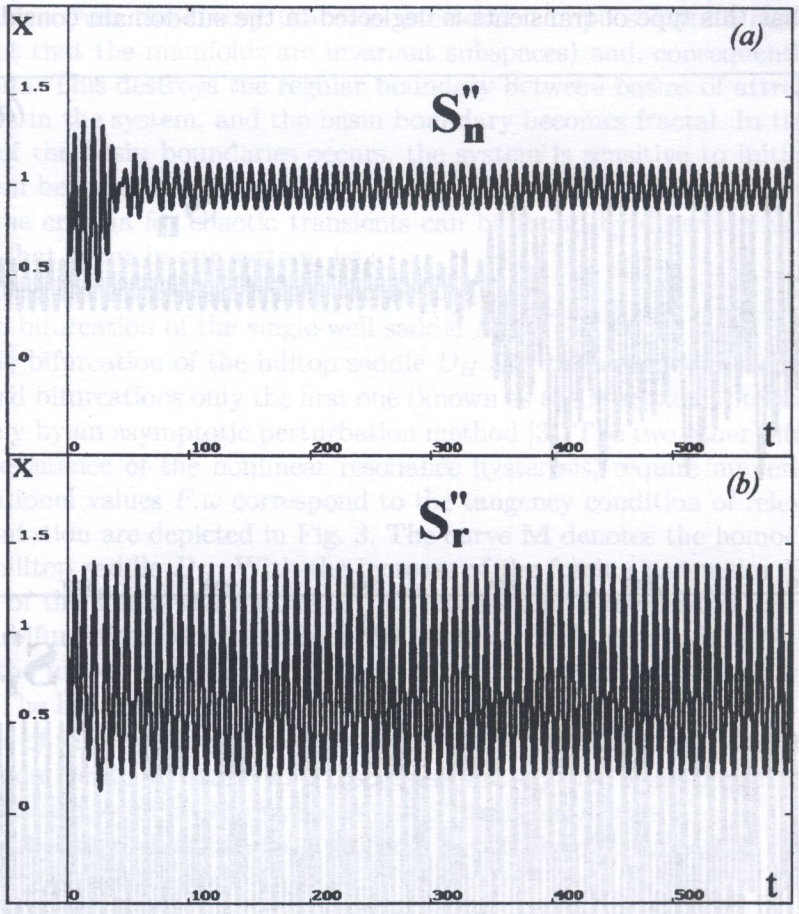

Fig. 8. Two time histories of the trajectories initializing at the smooth (non-fractal) domains of the basins of attraction, for the same control parameters as in Fig. 9: **(a)** $x(0) = 0.95$, $\dot{x}(0) = -0.36$ (basin of S_n''); **(b)** $x(0) = 0.90$, $\dot{x}(0) = -0.45$ (basin of S_r'')

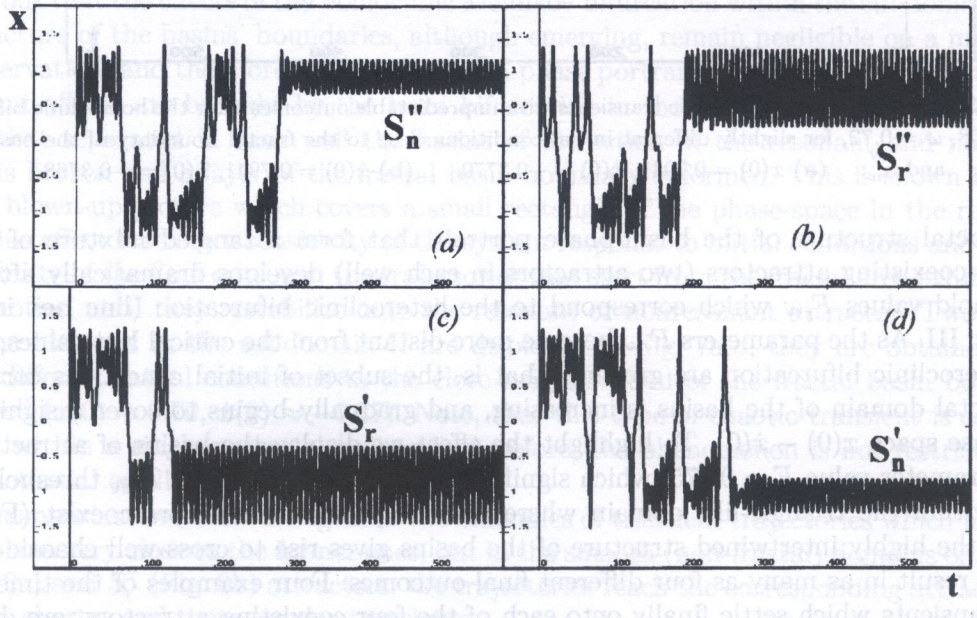

Fig. 9. Samples of cross-well chaotic transients with four unpredictable final outcomes at high forcing value, $F = 0.075$, with slightly different initial conditions: **(a)** $x(0) = 0.1100$, $\dot{x}(0) = -0.0090$; **(b)** $x(0) = 0.1102$, $\dot{x}(0) = -0.0088$; **(c)** $x(0) = 0.1099$, $\dot{x}(0) = -0.0090$; **(d)** $x(0) = 0.1097$, $\dot{x}(0) = -0.0095$

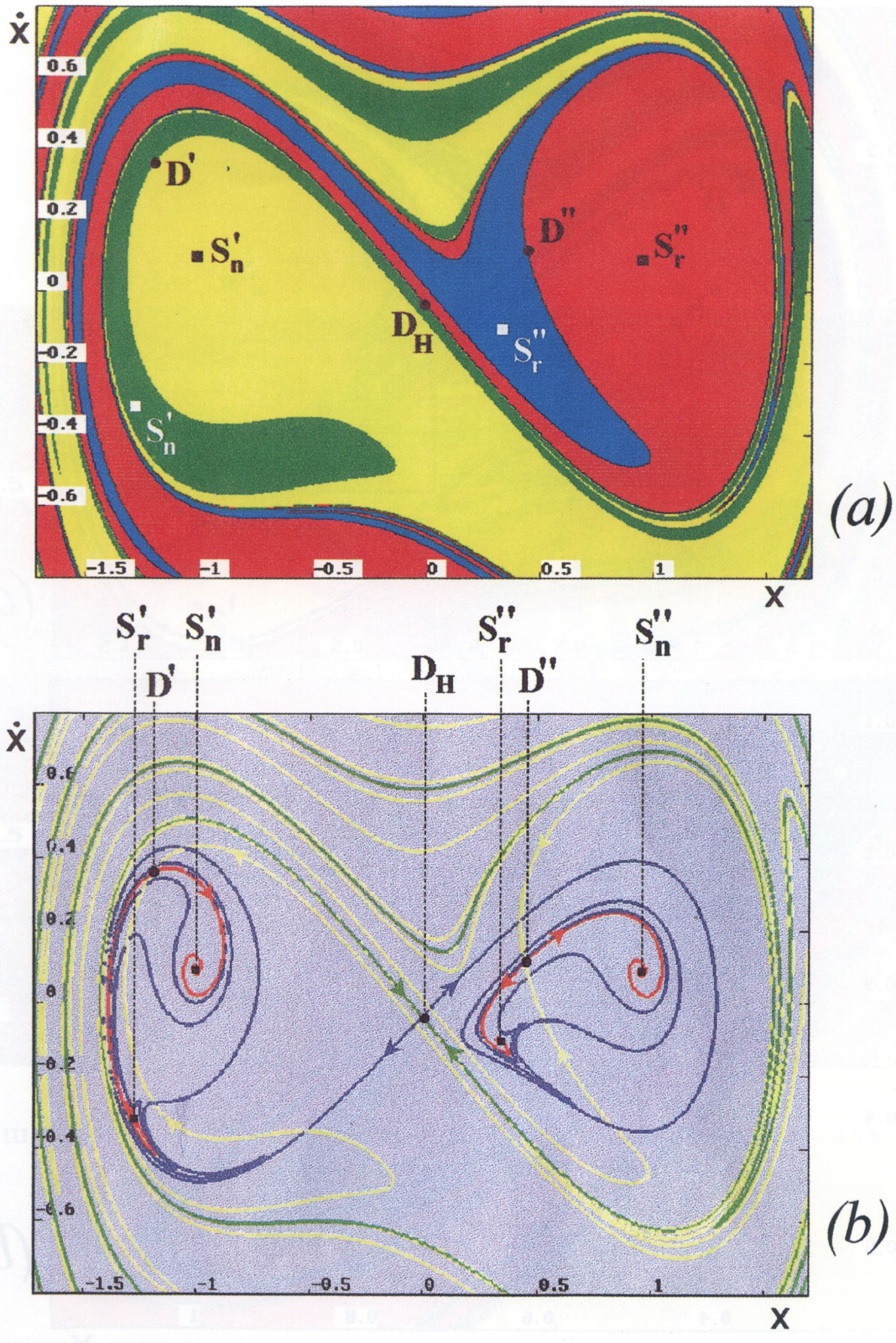

Fig. I. (a) Basins of attraction (in the $x - \dot{x}$ plane) of the four coexisting attractors, prior to any global bifurcation: $F = 0.05$, $\omega = 0.72$. Yellow depicts the basin of $S_n^{'}$, red – basin of $S_n^{''}$, green – basin of $S_r^{'}$, and blue – basin of $S_r^{''}$. The grid resolution is 640 x 480; **(b)** The corresponding family of invariant manifolds of the hilltop saddle D_H (insets in green, outsets in blue) and of the single-well saddles $D^{'}$, $D^{''}$ (insets in yellow, outsets in red)

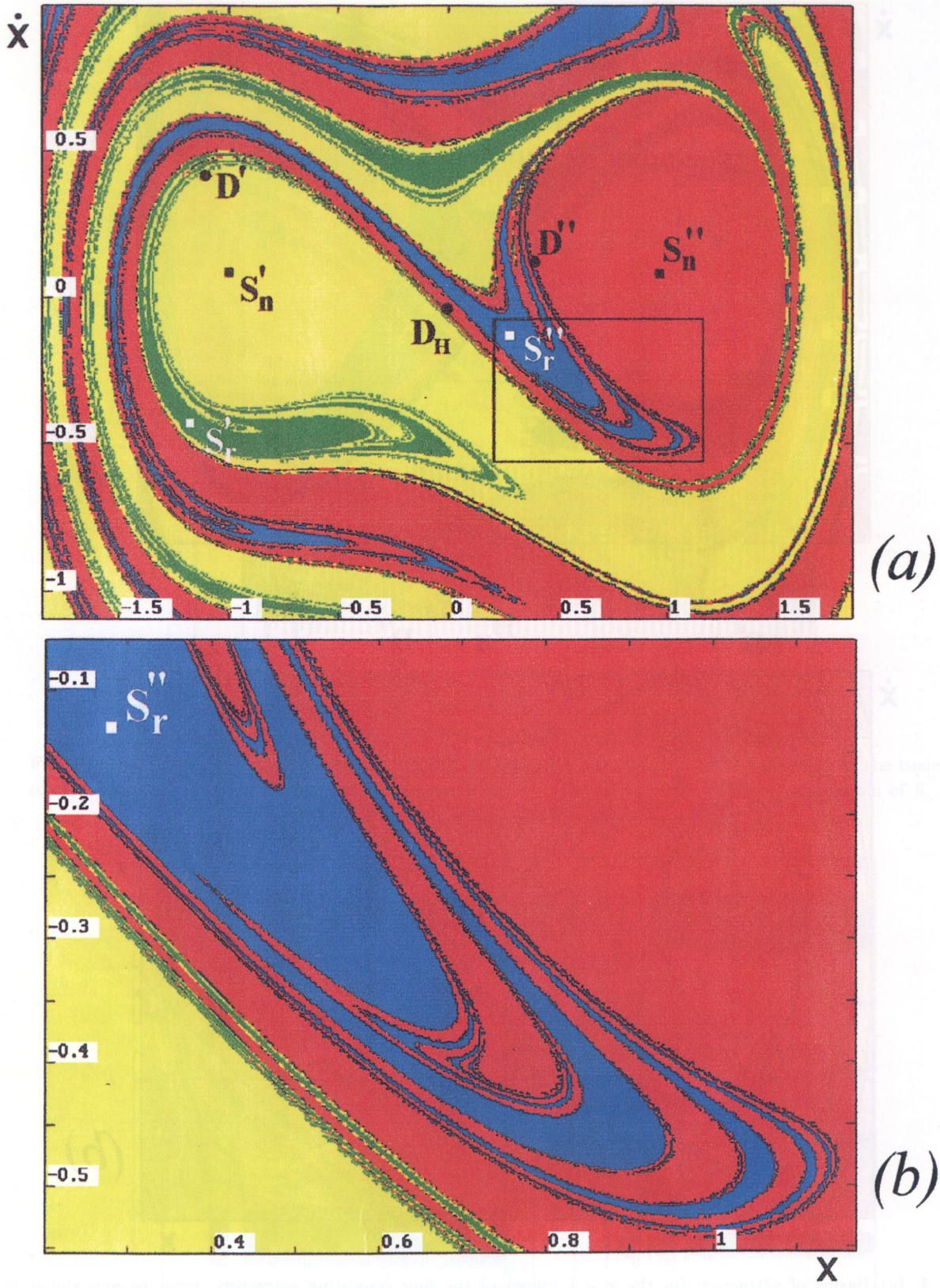

Fig. II. (a) Basins of attraction of the four coexisting attractors past the homoclinic bifurcation of the single-well saddles ($F_{\text{hom}} < F < F_{\text{het}}$): $F = 0.058$, $\omega = 0.72$; (b) Blown-up region of the basins (depicted as small rectangle in Fig. 10a) in the neighborhood of the S_r'' attractor. Color correspondence and grid resolution as in Fig. 6a

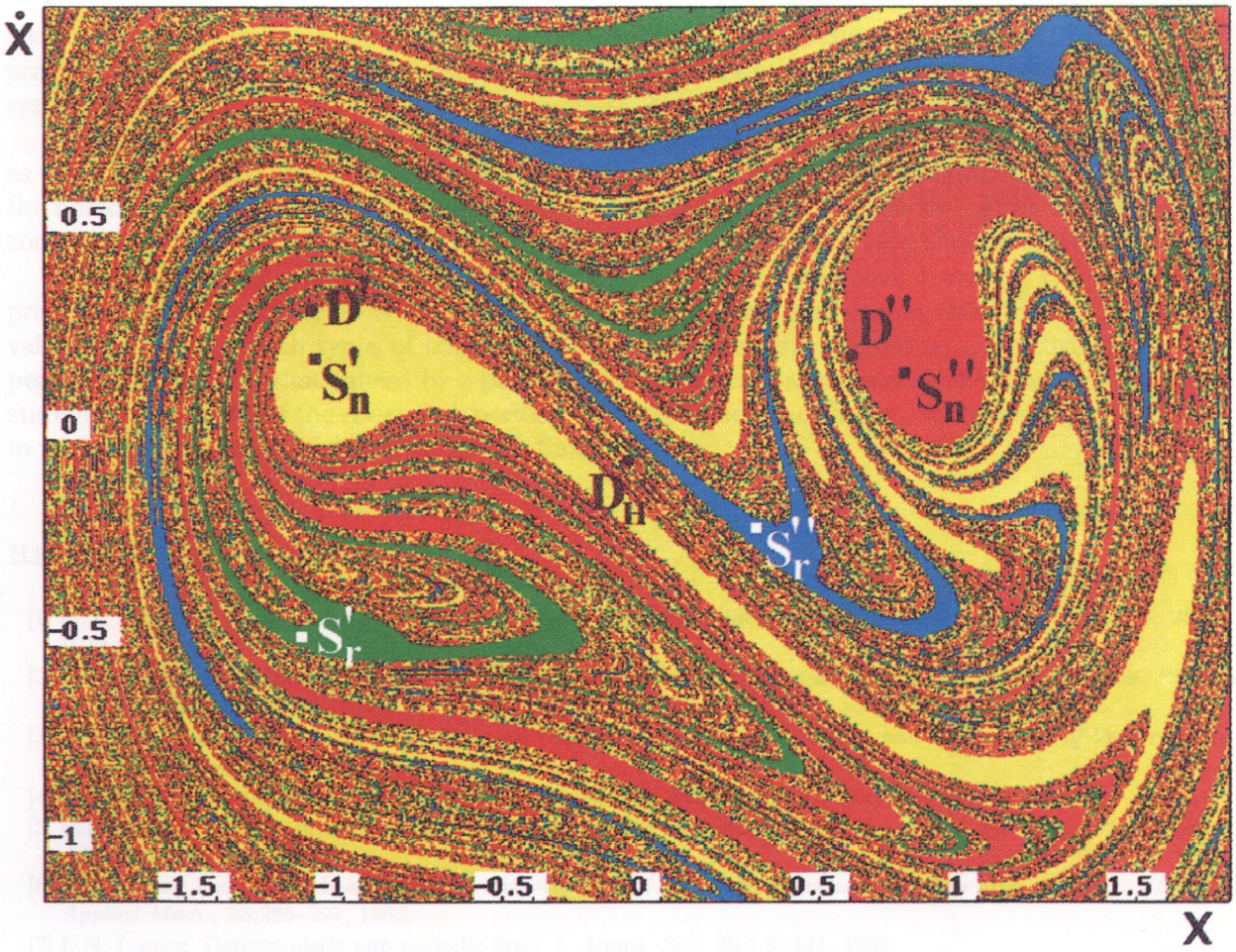

Fig. III. Basins of attraction of the four coexisting attractors at a higher value of forcing: $F = 0.075$, $\omega = 0.79$. Color correspondence and grid resolution as in Fig. 6a

When we turn back to the phenomena of transient chaos and indeterminate outcomes due to the disturbance of the control parameters F, ω at the stability limit of the periodic attractors (Figs. 4 and 5), we find out that also in this case the criteria for the chaotic transient are defined by the heteroclinic (**het**) bifurcation [19, 20, 24].

6. Conclusions

The numerical study of the criteria for chaotic transients in the mathematical model of buckled beams, i.e. the driven twin-well potential oscillator, leads to the following conclusions:

- the concept of maps plays an essential role in the computer based explorations, because it allows to reduce the three-dimensional phase space to the two-dimensional one. The graphical presentation of the results on the phase plane $(x, \dot{x})$ provides a key to clear interpretation of the system chaotic properties;
- application of the mathematical theory of global bifurcations in the system, where as many as three saddles associated with the four coexisting attractors give rise to occurrence of a series of the homoclinic and heteroclinic bifurcations, enables us to determine the loci of the critical system control parameters $F(\omega)$, which define the boundary between regular and chaotic system behavior;
- the criterion for the most dangerous phenomena — the cross-well transient chaos with unpredictable final outcome — is determined by the heteroclinic bifurcation (**het** in Fig. 3). For the values of $F > F_{\text{het}}$ both types of transient motion: the transient induced by a perturbation of the periodic motion, and that caused by a perturbation of control parameters in the close vicinity of the stability limit of one of the coexisting periodic attractors, become chaotic, with the unpredictability in both time of transient duration and its final outcome.

References

[1] M.J. Feigenbaum. Quantitative universality for a class of nonlinear transformations. *J. Stat. Phys.* **19**: 25-52, 1978.

[2] C. Grebogi, E. Ott and J.A. Yorke. Crises, sudden changes in chaotic attractors and transient chaos. *Physica* **D7**:181–200, 1983.

[3] J. Guckenheimer and P.J. Holmes. *Nonlinear Oscillations, Dynamical Systems and Bifurcations of Vector Fields.* Springer-Verlag, New York, 1983.

[4] Ch. Hayashi. *Nonlinear Oscillations in Physical Systems.* Princeton University Press, Princeton, N.J., 1985.

[5] P.J. Holmes. A nonlinear oscillator with a strange attractor. *Phil. Trans. of the Royal Soc. Lond.*, **A292**(1394):419–448, 1979.

[6] N.C. Huang and W. Nachbar. Dynamic snap-through of imperfect viscoelastic shallow arches. *Trans. ASME J. Applied Mech.*, **35**:286–297, 1968.

[7] E.N. Lorenz. Deterministic non-periodic flow, *J. Atmos. Sci.*, **20**:130-141, 1963.

[8] S.W. McDonald, C. Grebogi, E. Ott and J.A. Yorke. Fractal basin boundaries. *Physica* **D17**: 125–153, 1985.

[9] F.C. Moon. Experiments on chaotic motion of a forced nonlinear oscillator – strange attractors. *ASME J. of Applied Mechanics*, **47**:638–644, 1980.

[10] F.C. Moon. Experimental models for strange attractors: vibrations in elastic systems. In: *New Approach to Nonlinear Problems in Dynamics, SIAM*, 487–495, 1980.

[11] F.C. Moon. *Chaotic vibrations.* John Willey & Sons, New York, 1987.

[12] F.C. Moon and P.J. Holmes. A magnetoelastic strange attractor. *J. Sound and Vibrations*, **65**(2):275–296, 1979.

[13] H.E. Nusse and J.A. Yorke. *Dynamics: Numerical Explorations.* Springer-Verlag, New York, 1994.

[14] E. Ott. *Chaos in Dynamical Systems.* Cambridge University Press, Cambridge, 1993.

[15] M.S. Soliman. Jumps to resonance: Long chaotic transients, unpredictable outcome, and the probability of restabilization. *ASME J. Applied Mechanics*, **60**:669–676, 1993.

[16] H.B. Stewart and Y. Ueda. Catastrophes with indeterminate outcome. *Proc. Roy. Soc. Lond.*, **A432**:113–123, 1991.

[17] W. Szemplińska-Stupnicka and J. Rudowski. Steady-states in the twin-well potential oscillator: Computer simulations and approximate analytical studies. *CHAOS, Int. J. Nonlinear Science*, **3**(3):375–385, 1993.

[18] W. Szemplińska-Stupnicka and K.L. Janicki. Basin boundary bifurcations and boundary crisis in the twin-well Duffing oscillator: scenarios related to the saddle of the large resonant orbit. *Int. J. Bifurcation and Chaos*, **7**(1):129–146, 1997.

[19] W. Szemplińska-Stupnicka and E. Tyrkiel. Sequences of global bifurcations and the related outcomes after crisis of the resonant attractor in a nonlinear oscillator. *Int. J. Bifurcation and Chaos*, **7** (11), 1997.

[20] W. Szemplińska-Stupnicka and E. Tyrkiel. Sequences of global bifurcations and multiple chaotic transients in a mechanical driven oscillator, to be published in the *Proceedings of the IUTAM Symposium CHAOS'97*, Kluwer Academic Publishers, Dordrecht/Boston/London, 1997.

[21] J.M.T. Thompson and H.B. Stewart. *Nonlinear Dynamics and Chaos*. John Wiley & Sons, Chichester, 1986.

[22] J.M.T. Thompson, H.B. Stewart and Y. Ueda. Safe, explosive and dangerous bifurcations in dissipative dynamical systems. *Phys. Rev.*, **E 49**(2): 1019–1027, 1994.

[23] W.Y. Tseng and J. Dugundji. Nonlinear vibrations of a buckled beam under harmonic excitation. *ASME J. Applied Mechanics*, **36**: 467–476, 1971.

[24] E. Tyrkiel. Numerical exploration of post-bifurcation unpredictable outcomes in a nonlinear driven oscillator. In: *Proc. of the XIII Polish Conference on Computer Methods in Mechanics*, 1315-1322, Poznań University of Technology, Poznań, Poland, 1997.-

[25] Y. Ueda, S. Yoshida, H.B. Stewart and J.M.T. Thompson. Basin explosions and escape phenomena in the twin-well Duffing oscillator: compound global bifurcations organizing behavior. *Phil. Trans. Roy. Soc. London*, **A332**: 169–186, 1990.

[26] S. Wiggins. *Global Bifurcations and Chaos: Analytical Methods*. Springer-Verlag, New York, 1988.

[27] S. Wiggins. *Introduction to Applied Nonlinear Dynamical Systems and Chaos*. Springer-Verlag, New York, 1990.